Needle-Free Vaccine Injection

Mark A.F. Kendall

Contents

Abstract Millions of people die each year from infectious disease, with a main stumbling block being our limited ability to deliver vaccines to optimal sites in the body. Specifically, effective methods to deliver vaccines into outer skin and mucosal layers – sites with immunological, physical and practical advantages that cannot be targeted via traditional delivery methods – are lacking. This chapter investigates the challenge for physical delivery approaches that are primarily needle-free. We examine the skin's structural and immunogenic properties in the context of the physical cell targeting requirements of the viable epidermis, and we review selected current physical cell targeting technologies engineered to meet these needs: needle and syringe, diffusion patches, liquid jet injectors, and microneedle arrays/patches.

M.A.F. Kendall
Australian Institute for Bioengineering and Nanotechnology (AIBN), The University of Queensland, Building 75 – Cnr of College and Cooper Road The University of Queensland Brisbane, Brisbane, QLD4072, Australia
e-mail: m.kendall@uq.edu.au

M. Schäfer-Korting (ed.), *Drug Delivery*,
Handbook of Experimental Pharmacology 197,
DOI 10.1007/978-3-642-00477-3_7,

We then focus on biolistic particle delivery: we first analyze engineering these systems to meet demanding clinical needs, we then examine the interaction of biolistic devices with the skin, focusing on the mechanical interactions of ballistic impact and cell death, and finally we discuss the current clinical outcomes of one key application of engineered delivery devices – DNA vaccines.

Keywords Biolistics · DNA vaccines · Drug delivery · Gene guns · Immunotherapeutics · Langerhans cells · Skin · Skin mechanical properties · Microneedles · Vaccines

Abbreviations

A	Particle cross-sectional area
APC (APCs)	Antigen-presenting cell(s)
CST	Contoured shock tube
CHMP	Committee for Medicinal Products for Human Use
D	Particle resistive force
dDCs	Dermal dendritic cells
DEM	Discrete element model
DGV	Doppler global velocimetry
GMT	Geometric mean titer
HIV	Human immunodeficiency virus
PIV	Particle image velocimetry
RH	Relative humidity
SC	Stratum corneum
VE	Viable epidermis
V	Particle velocity
$v_{\mathrm{i,ve}}$	Viable epidermis boundary
ρ_{t}	Density of target
σ	Yield stress of target

1 Introduction

Vaccines are most commonly administered using a needle and syringe, a method first invented in 1853. The needle and syringe is effective, but unpopular, and creates a risk of iatrogenic disease from needle-stick injury or needle reuse as a consequence of the billions of administrations each year. Further, the needle and syringe does not deliver the vaccine ingredients optimally to the antigen-presenting cells (APCs), which alone can respond to the combination of antigen and adjuvant (innate immune stimulus) that makes a successful vaccine.

The provision of safe and efficient routes of delivery of vaccines to the immunologically sensitive dendritic cells in the skin (and mucosa) has the potential to

enhance strategies in the treatment of major diseases. The application of physical methods to achieving this goal presents unique engineering challenges in the physical transport of vaccines to these cells.

In this chapter, the physiology, immunology and material properties of the skin are examined in the context of the physical cell targeting requirements of the viable epidermis (as one example). Selected cell targeting technologies engineered to meet these needs are briefly presented. The operating principles of these approaches are described, together with a discussion of their effectiveness for the non-invasive targeting of viable epidermis cells and DNA vaccination against major diseases.

We then focus on one of these needle-free methods, called biolistics, that ballistically delivers millions of microparticles coated with biomolecules to outer skin layers. The engineering of these devices is presented, beginning with earlier prototypes before examining a more advanced system configured for clinical use. Then follows a theoretical and experimental analysis of the ballistic microparticle impact process, including the examination of induced cell death. Finally, the results of applying this technology to key human clinical trials are presented.

2 Targeting Skin and Mucosal Cells: The Immunological Rationale

Why are outer skin cells important targets in the treatment of disease? The answer is found from a consideration of skin structure, shown schematically in Figs. 1 and 2. Human skin can be subdivided into a number of layers: the outer stratum corneum (SC, 10–20 μm in depth), the viable epidermis (VE, 50–100 μm) and the dermis (1–2 mm) (Givens et al. 1993; Fuchs and Raghavan 2002). The SC is the effective physical barrier of dead cells in a "bricks and mortar" structure (Menton and Eisen 1971; Nemes and Steinert 1999). The underlying VE is composed of cells, such as immunologically sensitive Langerhans cells, keratinocytes, stem cells and melanocytes (Fuchs and Raghavan 2002). Unlike the dermis below, the VE lacks blood vessels and sensory nerve endings – important characteristics of a site for pain-free delivery with minimal damage.

In the VE, the skin has evolved a highly competent immunological function, with an abundance of Langerhans cells (500–1,000 cells mm^{-2}) (Berman et al. 1983; Chen et al. 1985; Stenn et al. 1992), often serving as the first line of defense against many pathogens (Babiuk et al. 2000). In particular, Langerhans cells (illustrated in Fig. 2) are extremely effective APCs, responsible for the uptake and processing of foreign materials in order to generate an effective immune response. Such cells are reported to be up to 1,000-fold more effective than keratinocytes, fibroblasts and myoblasts at eliciting a variety of immune responses (McKinney and Streilein 1989; Banchereau and Steinman 1998; Timares et al. 1998; Chen et al. 2002).

Less information is available on underlying, dermal APCs. New populations of dermal dendritic cells (dDCs) that express langerin (originally believed to be an

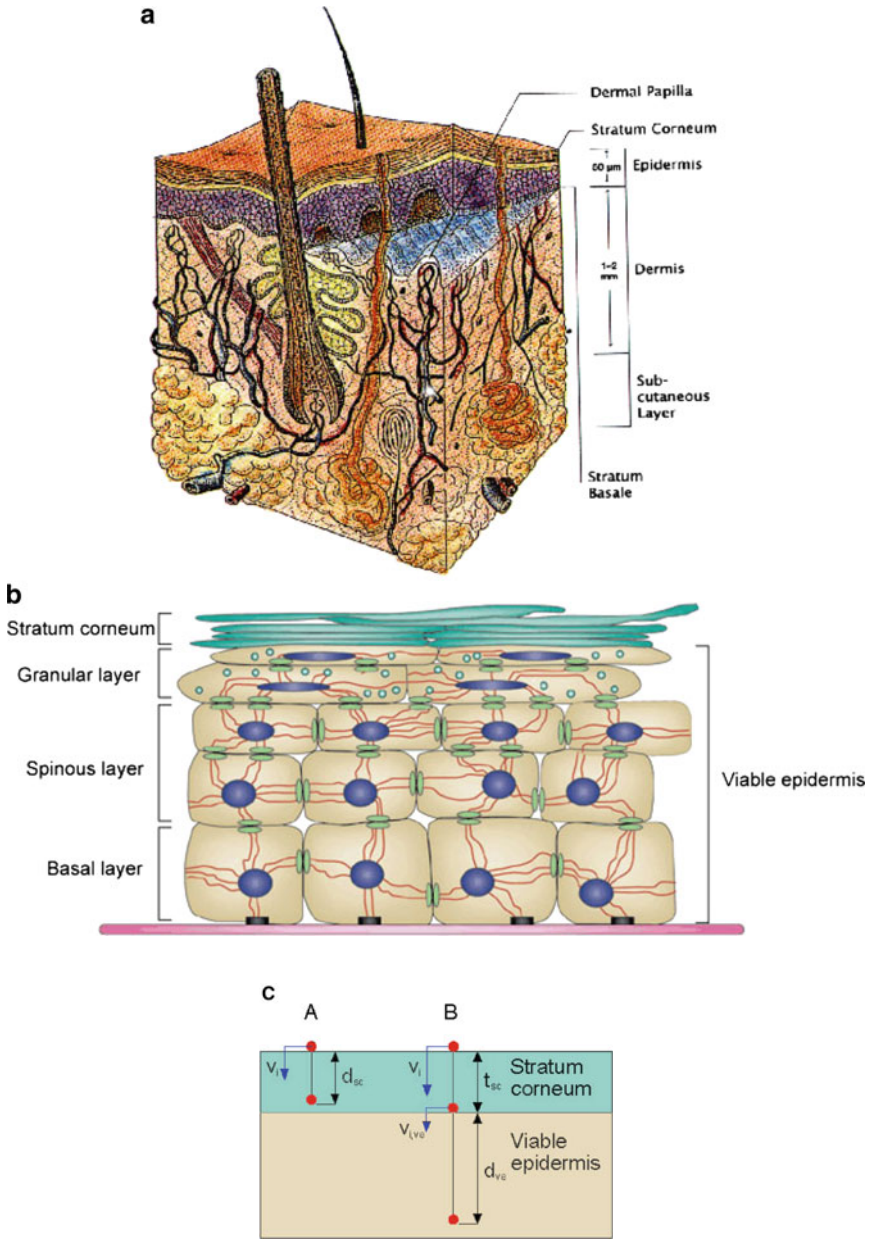

Fig. 1 A schematic diagram of the structure of mammalian skin (**a**), the epidermis of mammalian skin (**b**), and the corresponding bilayer approximation of the epidermis used for the theoretical penetration model (**c**). Penetration case A denotes particle delivery into the stratum corneum (d_{sc}), whereas, in case B, the stratum corneum is fully breached (t_{sc}) and the final particle location is within the viable epidermis (d_{ve}). The impact velocity is v_i, whilst the input velocity for the viable epidermis is $v_{i,ve}$. Adapted from Kendall et al. (2004b)

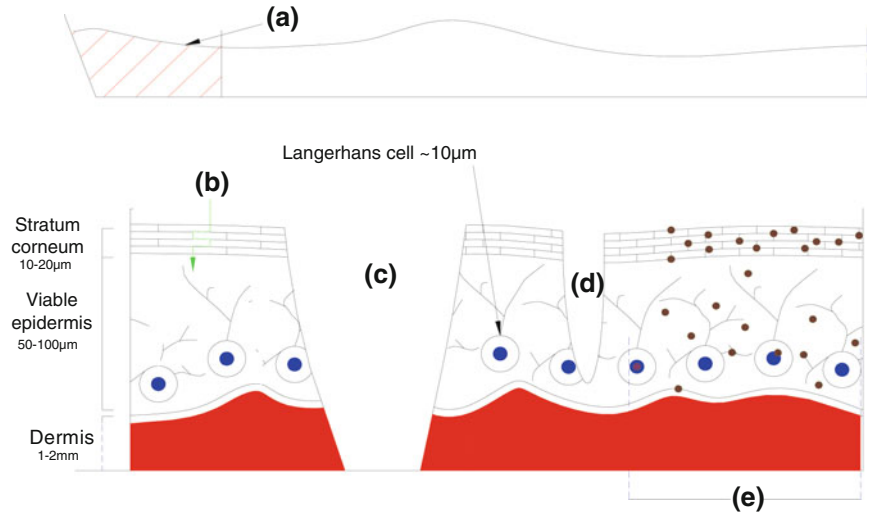

Fig. 2 A schematic cross-section of the skin showing Langerhans cells. Five physical cell targeting approaches are also shown. (**a**) A half-section of a small gauge needle and syringe; (**b**) route of diffusion from patches; (**c**) penetration from a liquid jet injector; (**d**) a hole from a microinjector; and (**e**) distribution of microparticles following biolistic injection. From Kendall (2006)

exclusive marker for Langerhans cells) reportedly exist (Poulin et al. 2007) and have unique immunological functions within the skin (Nagao et al. 2009). Thus, directly targeting specific Langerhans cells or dermal APC populations will allow immune responses to be modulated following vaccination.

For simplicity, this chapter focuses on delivery methods targeting vaccine to the most defined skin APC population, the Langerhans cells, residing in the epidermis. Effective in situ (in vivo) targeting of Langerhans cells and other epidermal cells with polynucleotides or antigens will open up novel applications in disease control (Chen et al. 2002), including vaccination against major viruses/diseases, such as human immunodeficiency virus (HIV) and cancer.

3 Engineering of Physical Approaches for the Targeting of Skin and Mucosal Cells

Within the VE, the location of Langerhans cells – as a delivery target for immunotherapeutics – is tightly defined by:

- A vertical position at a consistent suprabasal location (Hoath and Leahy 2002);
- A spatial distribution in the horizontal plane evenly distributed throughout the skin (Numahara et al. 2001);

- A constitution of 2% of the total epidermal cell population (in human skin) (Bauer et al. 2001).

Despite its recognized potential, the VE has only recently been viewed as a feasible cellular targeting site with the emergence of new biological and physical technologies. The challenge is the effective penetration of the SC and precise targeting of the cells of interest.

3.1 Mechanical Properties of the SC Barrier

The SC is a semi-permeable barrier that, owing to its variable mechanical properties, is challenging to breach in a minimally invasive manner, to target the viable epidermal cells below. Mechanically, the SC is classified as a bio-viscoelastic solid and shows highly variable properties. Obvious differences include the huge variation in thickness and composition with the skin site and the age of an individual (Hopewell 1990). However, there are more subtle and equally important variations in SC properties to consider when configuring targeting methods.

For example, the SC mechanical breaking stress is strongly influenced by the ambient humidity/moisture content (Wildnauer et al. 1971; Christensen et al. 1977; Rawlings et al. 1995; Dobrev 1996; Nicolopoulos et al. 1998) – the relative humidity range from 0% to 100% results in a decrease in excised human SC breaking stress from 22.5 to 3.2 MPa (Kendall et al. 2004b). Similarly, an increase in ambient temperature also results in an SC breaking stress decrease by an order of magnitude (Papir et al. 1975).

More recently, with indentation studies using small probes (diameters of 2 and 5 μm) fitted to a NANO-Indenter (Kendall et al. 2007), we have found more complexity and variation in key SC, and underlying VE, mechanical properties. Specifically:

- The storage modulus and mechanical breaking stress both dramatically decrease through the SC (Fig. 3a, 3b);
- At a given depth within the SC and VE, decreasing the probe size significantly increases the storage modulus (Fig. 3a).

These and other sources of variability in the SC mechanical properties present challenges in configuring approaches to breach the SC in a minimally invasive manner, and effectively deliver vaccines to the underlying cells.

3.2 Biological Approaches

Although the focus of this chapter is on physical approaches to target epidermal cells, it is also important to highlight biological approaches. A powerful biological approach to the transport of biomolecules to epidermal (and other) cells, in vivo, exploits the evolved function of viruses in the transport to cells. In gene delivery,

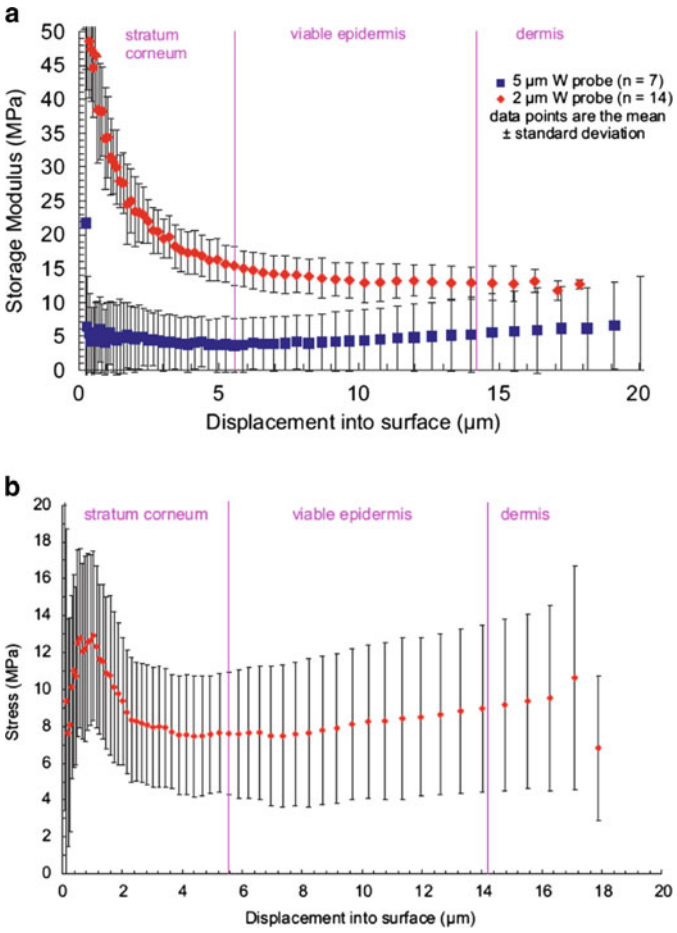

Fig. 3 Mechanical properties (mean ± standard deviation) as a function of displacement obtained with microprobes indented into murine ears. (**a**) Storage modulus with 5 and 2 μm microprobes. (**b**) Stress with a 2 μm microprobe. Adapted from Kendall et al. (2007)

researchers have made use of genetically engineered viruses in DNA vaccination and gene therapy of major diseases with encouraging results; however, viral gene delivery is hindered by safety concerns, a limited DNA-carrying capacity, production and packaging problems and a high cost (Lu et al. 1997; Tang et al. 1997).

3.3 Physical Cell Targeting Approaches

Alternatively, many physical technologies are being developed. Potentially, they can overcome some limitations of biological approaches using needle-free

mechanisms to breach the SC barrier to facilitate drug and vaccine administration directly to epidermal cells. Figure 2 illustrates schematically key physical targeting approaches relative to the scale of typical skin and the Langerhans cell layer of interest.

Needle and syringe. The most common physical delivery method, a small gauge needle and syringe, is shown in half-section in Fig. 2a. Although this approach easily breaches the SC, precise targeting of the Langerhans cell-rich VE cannot be practically achieved. Hence, the needle and syringe is used for intradermal or intramuscular injection. This inefficient, indirect targeting of dendritic cells with DNA has resulted in modest immune responses (Mumper and Ledebur 2001). Other disadvantages of the needle and syringe include risks due to needle-stick injuries (WHO 1999) and needle phobia (Givens et al. 1993).

Diffusion/permeation delivery. The least invasive method of breaching the SC is probably by permeation through it, driven by diffusion from patches applied to the skin (Fig. 2b) (Glenn et al. 2003). However, the current general view is that this mode of delivery is best suited to smaller biomolecules (<500 Da) (Glenn et al. 2003) – considerably smaller than vaccines. This view is being challenged, with a recent study showing that very large recombinant antigens of ~1 MDa can be delivered to elicit systemic responses by diffusion from patches (Guerena-Burgueno et al. 2002). The transport of larger biomolecules through the SC can be further enhanced by simple approaches, including tape stripping with an adhesive tape, brushing with sandpaper (Liu et al. 2001; Watabe et al. 2001) or the application of depilatory agents (Tang et al. 1997; Shi et al. 1999, 2001). Amongst the more advanced technologies are electroporation (Widera et al. 2000; Zucchelli et al. 2000), ablation by laser or heat, radiofrequency high-voltage currents (Sintov et al. 2003), iontophoresis (Alexander and Akhurst 1995; Li and Hoffman 1995; Domashenko et al. 2000), sonophoresis and microporation (Babiuk et al. 2000). Many of these approaches remain untested for complex entities such as vaccines and immunotherapies. Permeation through the SC can also be enhanced by the coating of plasmid DNA on nanoparticles (~100 nm) for DNA vaccination (Cui and Mumper 2001).

Liquid jet injectors. Interest in using high-speed liquid jet injectors arose in the mid-twentieth century because of its needle-free approach (Furth et al. 1995). This technique has seen a recent resurgence, with liquid delivered around the Langerhans cells in gene transfer and DNA vaccination experiments (Furth et al. 1995), and the delivery of drugs (Bremseth and Pass 2001). As shown in Fig. 2c, current liquid jet injectors typically disrupt the skin in the epidermal *and* dermal layer. To target exclusively the viable epidermal cells, such as Langerhans cells, the challenge of more controlled delivery needs to be addressed. With the dermal disruption induced by administration, liquid jet injectors are also reported to cause pain to patients.

Microneedle arrays/patches. Researchers have overcome some of the disadvantages described by fabricating arrays of micrometer-scale projections to breach the SC and to deliver naked DNA to several cells in live animals (Mikszta et al. 2002). Similar microprojection devices are used to increase the permeability of drugs

(Matriano et al. 2002) and "conventional" protein antigen vaccines (Matriano et al. 2002; McAllister et al. 2003). Figure 2d shows that, unlike current liquid jet injectors, these microneedles can accurately target the VE. Furthermore, they are as simple to use as patches, whilst overcoming the SC diffusion barrier to many molecules. Moreover, compared with both the needle and syringe and liquid jet injectors, these microneedle methods are pain-free because of epidermal targeting. By drawing upon a range of manufacturing techniques, McAllister et al. (2003) have shown that these microneedle arrays can be made from a range of materials, including silicon, metal and biodegradable polymers.

Newer devices are now being tailored to the immunological problem of *directly* targeting vaccines to the skin APC. One example is micro-nanoprojection array (otherwise called "nanopatches"). Nanopatches (Chen et al. 2008, 2009; Prow et al. 2008) are very small and densely packed on patches (less than 100 μm in length and over 20,000 MPs cm^{-2}), clearly distinct from the large and sparsely packed ones reported in literature (up to 700 μm in length and less than 321 projections per cm^2) (Matriano et al. 2002; Gill and Prausnitz 2007). These configurations produce highly-targeted and unique immune responses in mice. This includes, in the animal model:

- Orders of magnitude in vaccine dose reduction, compared to the needle and syringe while achieving an equivalent immune response (data submitted for publication) following the delivery of existing conventional vaccines;
- Greatly enhanced immune responses and vaccination protection against disease, obtained by nanopatch delivery of candidate DNA-based vaccines (compared to needle and syringe intradermal delivery).

Importantly, nanopatches are also practical devices – cheap to manufacture, with dry-coated vaccines stable at ambient temperature (i.e., not requiring refrigeration) and easy to use.

4 Biolistic Microparticle Delivery

Currently, the most established physical method of DNA vaccination is biolistic microparticle delivery, otherwise known as gene guns (Fig. 2e); this is the focus of the remainder of the chapter.

4.1 Biolistics Operating Principle

In this needle-free technique, pharmaceutical or immunomodulatory agents, formulated as particles, are accelerated in a supersonic gas jet to sufficient momentum to penetrate the skin (or mucosal) layer and to achieve a pharmacological effect.

Sanford et al. (1987) pioneered this innovation with systems designed to deliver DNA-coated metal particles (of diameter of the order of 1 μm) into plant cells for genetic modification, using pistons accelerated along the barrels of adapted guns (Sanford and Klein 1987). The concept was extended to the treatment of humans with particles accelerated by entrainment in a supersonic gas flow (Bellhouse et al. 1994). Prototype devices embodying this concept have been shown to be effective, painless, and applicable to pharmaceutical therapies ranging from protein delivery (Burkoth et al. 1999), to conventional vaccines (Chen et al. 2000) and DNA vaccines (Roy et al. 2000; Lesinski et al. 2001).

Different embodiments of the concept (e.g., in Figs. 4 and 5) all have a similar operating procedure. Consider the prototype shown schematically in Fig. 4a as one example. Prior to operation, the gas canister is filled with helium or nitrogen to 2–6 MPa and the vaccine cassette, comprising two 20 μm diaphragms, is loaded with a powdered pharmaceutical payload of 0.5–2 mg. The pharmaceutical material is placed on the lower diaphragm surface. Operation commences when the valve in the gas canister is opened to release gas into the rupture chamber, where the pressure builds up until the two diaphragms retaining the vaccine particles sequentially burst. The rupture of the downstream diaphragm initiates a shock which propagates down the converging−diverging nozzle. The ensuing expansion of stored gas results in a short-duration flow in which the drug particles are entrained and accelerated through the device. After leaving the device, particles impact on the skin and penetrate to the epidermis to induce a pharmacological effect.

4.2 Engineering of Hand-Held Biolistic Devices for Clinical Use

Biolistic delivery of immunotherapeutics is an application of transonic flow technology that is otherwise applied to aerospace applications. In this section we introduce prototype devices and discuss the key engineering challenges in applying this aerospace technology to clinical applications. Key parameters used to guide the engineering of biolistic devices are:

- A nominally uniform, controlled and quantified microparticle velocity and spatial distribution impacting the tissue target. Further, the impact momentum is to be within the range needed for delivery to particular locations (e.g., the Langerhans cells for DNA vaccines).
- A sufficient “footprint” on the tissue to deliver sufficient payload and target the appropriate number of cells.
- Noise levels within the user guidelines, for both the operator and patient.
- The device is to be hand-held.
- For long-term stability, the pharmaceutical is to be stored within a sealed environment.
- The device is to be produced from biocompatible materials.

- The devices, manufactured in large numbers, are to be cost-competitive with other relevant technologies.

Earlier generation systems attempting to address these parameters used a prototype device family generated from empirical studies. A schematic of one of these devices, using a convergent−divergent nozzle design is shown in Fig. 4a (Kendall et al. 2004c). Working with these devices, the challenge was to establish the gas−particle dynamics behavior of the systems. A significant research program was directed at this goal.

An array of methods were used to characterize the gas and particle dynamics of these systems. Quinlan et al. (2001) performed static pressure measurements to interrogate the gas flow, together with time-integrated Doppler Global Velocimetry (DGV) measurements of drug particle velocity (Quinlan et al. 2001). These measurements were very useful, but gave an incomplete description of the predominantly unsteady flow in the device.

In subsequent broader studies, the transient gas and particle flow within the device were interrogated with Pitot-static pressure measurement (as instrumented in Fig. 4a), together with Schlieren imaging, and time resolved DGV (Quinlan et al. 2001) and computational fluid dynamics (CFD) modeling (Liu and Kendall 2004b). The findings of this study are summarized with measured axial Mach number profiles through the nozzle (Fig. 4b) and a single Schlieren image (Fig. 4c).

The axial profiles of Mach number at various times after termination of the starting process (based on total-static and Pitot-static pressure measurements) are compared with the theoretical Mach number profile for steady isentropic quasi-one-dimensional supersonic flow (with the assumption of a choked throat) in Fig. 4b. Pitot and static pressure measurements (p_2 and p_3 respectively in Fig. 4a) suggest that 500 μs after diaphragm rupture, the flow 38.5 mm upstream of the nozzle exit is supersonic and close to the isentropic ideal. Further downstream, however, the overexpanded nozzle flow is processed through an oblique shock system which induces flow separation. Consequently, the experimentally determined Mach number (determined from Pitot and static pressure) gradually falls from between 2 and 2.5 (23.5 mm upstream of the exit plane) to 1.5 at the exit plane. The Mach number in the downstream region of the nozzle decays with time as the shock system moves upstream.

Sequences of Schlieren images such as the sample shown in Fig. 4c (t = 132 μs) reveal the structure of the evolving flowfield with greater detail and clarity (Kendall et al. 2004c). The oblique shocks visible have evolved to form at least three oblique shock cells that have interacted with the boundary layer and separated the nozzle flow. DGV images show particles were entrained in the nozzle starting process and the separated nozzle flow – regimes with large variations in gas density and velocity – giving rise to large variations in particle velocity (200–800 m s^{-1}) and spatial distributions (Kendall et al. 2004c). Clearly, the first criterion from above is not satisfied with this geometry.

Furthermore, the gas flow throughout much of the nozzle (Fig. 4c) is highly sensitive to variations in the nozzle boundary condition imposed by inserting a

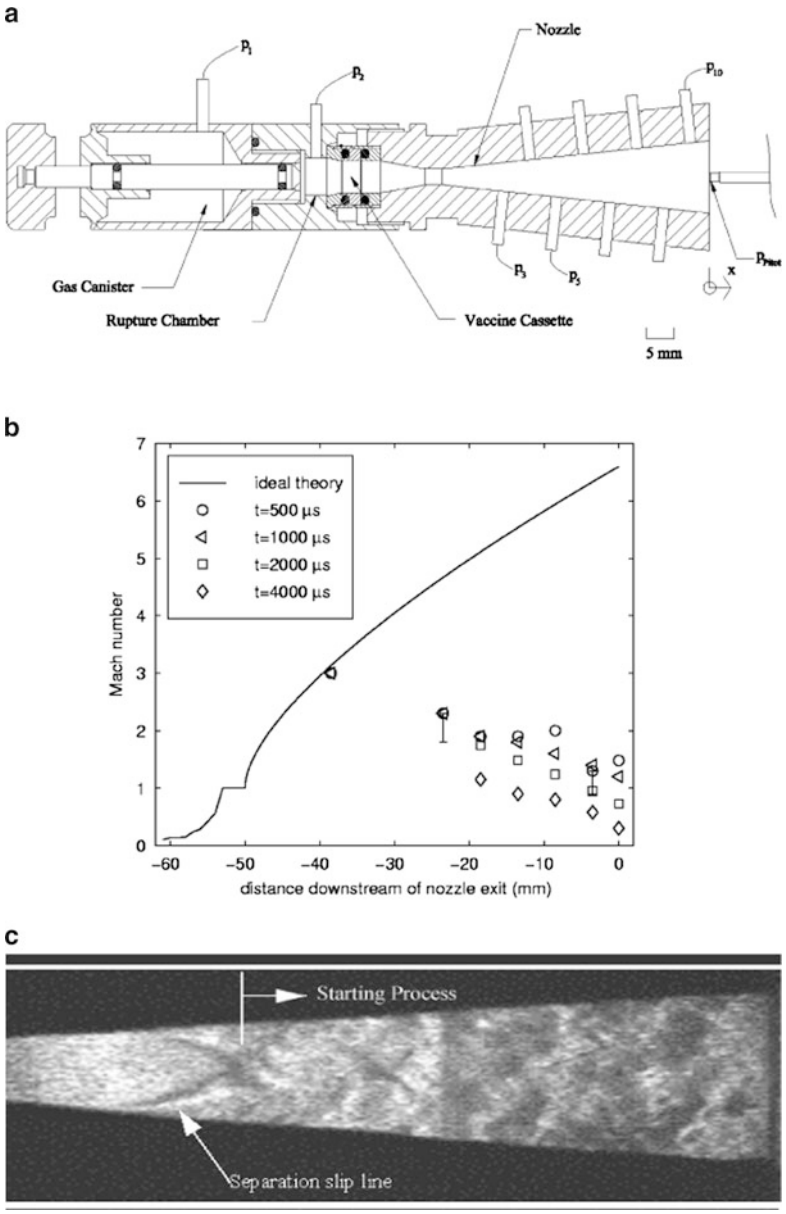

Fig. 4 (**a**) Schematic of a simplified prototype vaccine device instrumented for Pitot and static pressure measurements. The static pressure transducers are labeled p_1–p_{10}. (**b**) Experimental and ideal axial Mach number within the conical nozzle of investigation. The profiles are provided after the starting process. (**c**) A sample Schlieren image within the nozzle. From Kendall et al. (2004c)

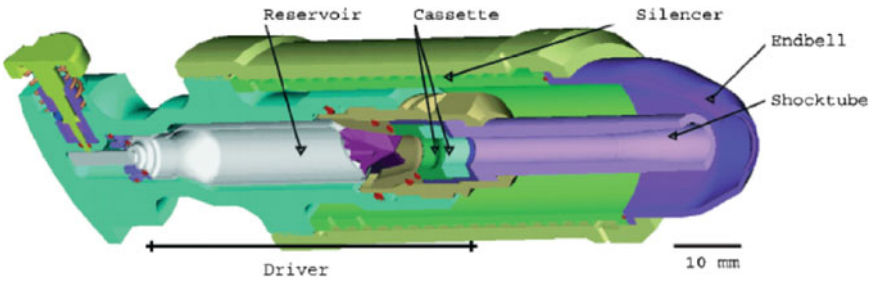

Fig. 5 A contoured shock tube (CST) prototype configured for clinical biolistic delivery. From Kendall (2002)

tissue target and/or a silencer – because the boundary condition information can be communicated upstream. This means that this silenced device applied to the tissue target would have considerably lower and more variable impact velocities. In some cases, it is questionable whether these subsonic nozzle flow silenced devices would deliver particles with a sufficient momentum to reach the target tissue layer.

Improved devices for clinical use to overcome the large variations in particle impact conditions in described earlier devices, and meet the other important criteria of a practical clinical system (outlined above), a next generation biolistic device, called the Contoured Shock Tube (CST) (Fig. 5), was conceived and developed (Kendall 2002; Liu and Kendall 2004a; Hardy and Kendall 2005; Marrion et al. 2005; Truong et al. 2006; Liu et al. 2007). The devices operate with the principle of delivering a payload of microparticles to the skin with a narrow range of velocities, by entraining the drug payload in a quasi-one-dimensional, steady supersonic flowfield.

In experiments with simple prototype CST devices, it was shown that the desired gas flow was achieved repeatedly (Kendall 2002). Importantly, further work with particle payloads measured a variation in free-jet particle velocity of $\pm$ 4% (Kendall et al. 2006). In this research, measurements were made with Particle Image Velocimetry (PIV). A sample PIV result is shown in Fig. 6. Similar PIV images at a range of times after diaphragm rupture were processed to extract the mean centerline axial particle velocity profiles. Importantly, these PIV measurements show particle payloads do achieve near uniform exit-plane velocities at the device exit over the time interval studied. This CST device prototype was a benchtop prototype, not addressing the key criteria for a practical, hand-held clinical immunotherapeutic system.

An embodiment of the CST configured to meet these clinical needs is shown in Fig. 5, with the key components labeled. The device was fabricated from biocompatible materials and the device wall thickness was kept relatively constant to meet autoclave sterilization requirements. To reduce the overall system length, the bottle reservoir (which operates by an actuation pin) is located within the driver annulus. A challenge of this co-axial arrangement was to maintain integrity of transonic gas flow within the driver initiated after diaphragm rupture. This challenge was met by

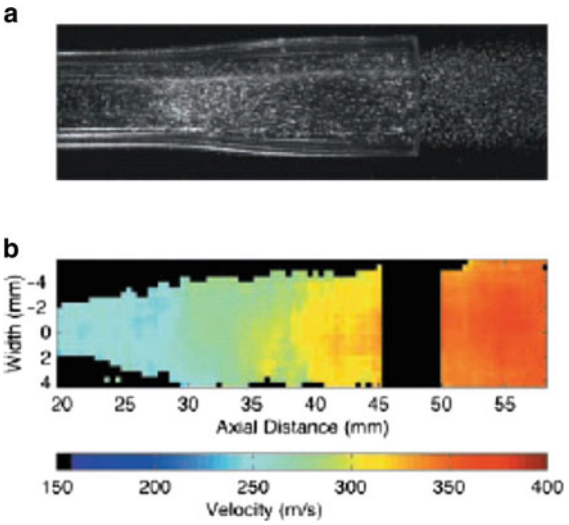

Fig. 6 A raw image (**a**) and derived Particle Image Velocimetry velocity map (**b**) of the instantaneous particle flowfield of a CST prototype, taken 225 μs after diaphragm rupture. The payload was 2.2 mg of 39 μm diameter polystyrene spheres. From Kendall (2002)

carefully contouring the driver and obstacle of the mounting arrangement (Marrion et al. 2005). Possible fragments from opening of the aluminium gas bottle are contained by a sealed filter at the bottle head.

The powdered pharmaceutical is enclosed and sealed by a cassette created by the inclusion of additional diaphragms upstream of the particle payload. In this case, the cassette houses two jets designed to mix the particles into a cloud, hence reducing the dependence on the initial particle location (Kendall 2002; Truong et al. 2006). Therefore, a nominally uniform spatial distribution of particles is released within the quasi-steady flow through the shock tube and nozzle. Repeated in vitro and in vivo experiments show that polycarbonate diaphragm fragments do not damage the target.

Elements of the silencing system are also shown in Fig. 5. The primary shock initiated by diaphragm rupture, reflected from the target, is identified as the main source of sound to be attenuated. This shock is collapsed into compression waves by a series of compressions–expansions induced by an array of orifices and saw-tooth baffles, resulting in appropriate sound levels for the operator and patient.

The device lift-off force is also to be well within user constraints. A peak lift-off force of 13 N is achieved by the careful selection of endbell contact diameter, silencer volume, flow rates through the reservoir and silencer geometry. This peak was for only a very short time within a gas flow lasting only ~200 μs (with a helium driver gas). The point of contact between the device and skin target was selected to maintain a target seal and to minimize the lift-off force, whilst not adversely affecting the impact velocities of the particles. The effect of silencing was also minimized by maintaining a supersonic gas flow transporting particles through the nozzle – so changes in the nozzle boundary condition were not fed upstream. The range of impact conditions for the CST platform was achieved by the selection

of appropriate helium/nitrogen mixtures within the gas bottle driver/driven area ratios.

4.3 Ballistics Microparticle Delivery to Skin

We now examine delivery of microparticles from these quantified and highly-controlled biolistics devices, impacting the skin. Figure 1 shows that skin is a highly variable, bio-viscoelastic material.

The described biolistic devices have been applied to a range of tissue targets for immunotherapeutic applications, including the skin of rodents (Kendall et al. 2006), pigs (Kendall et al. 2004b), dogs (Mitchell 2003), and humans (Kendall et al. 2004a). Typically, two classes of particles are delivered to the tissue. In the powder delivery of conventional vaccines and allergens for allergy immunotherapy, particles of 10–20 μm in radius are delivered to the epidermis of the skin to achieve a therapeutic effect (Kendall 2006). DNA vaccination, however, is an application in which smaller (radius 0.5–2 μm) gold particles coated with a DNA construct are targeted at the nuclei of key immunologically sensitive cells within the epidermis (Lesinski et al. 2001).

4.3.1 Theoretical Model for Ballistic Impact into Skin

In these particle impact studies, the mechanisms of particle impact were explored with a theoretical model, based on a representation first proposed by Dehn (Dehn 1976). The model attributes the particle resistive force (D) to plastic deformation and target inertia

$$D = \frac{1}{2}\rho_t A v^2 + 3A\sigma, \tag{1}$$

where ρ_t and σ are the density and yield stress of the target, A is the particle cross-sectional area and v is the particle velocity. The yield stress (sometimes known as the breaking stress) is the stress at which the tissue begins to exhibit plastic behavior. Equation (1) may be integrated to obtain the penetration depth as a function of particle impact and target parameters. The key parameters of the skin used in the model are summarized in Table 1. Note that these parameters have all been obtained at low, quasi-static strain rates and not the high ballistic strain rates.

The theoretical model of particle penetration into the epidermis using Eq. (1) in a two-layer model is shown in Fig. 1c. Expression (1) shows that the yield stress and density of the SC and VE are important in the ballistic delivery of particles to the epidermis.

In the case of particle delivery only to the SC (labeled "A" in Fig. 1c), the particle depth into the SC (d_{sc}) is obtained by the integration of Eq. (1)

Table 1 Parameters and assigned values used in the theoretical calculations of the particle penetration depth as a function of the relative humidity. From Kendall et al. (2004b)

Skin region	Parameter	Value	Source
Stratum corneum	σ_{sc} (MPa)	22.5–3.2 (0%–100% RH)	Wildnauer et al. (1971)
	ρ_{sc} (kg m^{-3})	1,500	Duck (1990)
	t_{sc} (μm)	10–15.6 (0%–93% RH)	Blank et al. (1984) and measurement
Viable epidermis	σ_{ve} (MPa)	2.2	actin tensile, Kishino and Yanagida (1988)
		10	Epithelium, Mitchell et al. (2003)
	ρ_{ve} (kg m^{-3})	1,150	Duck (1990)

$$d_{sc} = \frac{4\rho r}{3\rho_{sc}}\left\{\ln\left(\frac{1}{2}\rho_{sc}{v_i}^2 + 3\sigma_{sc}\right) - \ln(3\sigma_{sc})\right\}, \tag{2}$$

where the subscript sc denote the SC. Also, v_i and σ_{sc} are, respectively, the particle impact velocity and SC yield stress.

If the particle impact momentum is sufficient to breach the SC (labeled "B" in Fig. 1c), Eq. (2) is rearranged to obtain the velocity of the particle at the SC−VE boundary ($v_{i,ve}$), i.e.,

$$v_{i,ve} = \left\{\left(v_i^2 + \frac{6\sigma_{sc}}{\rho_{sc}}\right)\exp\left(-\frac{3\rho_{sc}t_{sc}}{4\rho r}\right) - \frac{6\sigma_{sc}}{\rho_{sc}}\right\}^{1/2}, \tag{3}$$

where t_{sc} is the thickness of the SC.

The subsequent particle penetration in the VE (d_{ve}) is then calculated using Eq. (2), using instead the material properties of the VE and $v_{i,ve}$. The total particle penetration depth (d_t) is thus

$$d_t = t_{sc} + d_{ve}. \tag{4}$$

An alternative fully numerical Discrete Element Model (DEM) approach has also been applied (Mitchell et al. 2003), but will not be discussed here.

4.3.2 Locations of Microparticles into Skin

As an example, particle delivery to excised human skin is shown for both classes of particles in Fig. 7 (Kendall et al. 2004a). In Fig. 7a, a glass particle of 20 μm radius delivered to the skin at a nominal entry velocity of 260 m s^{-1} is shown. Note the variation in both the SC and epidermal thicknesses. Histological sampling of the three skin sites is from the backs of cadavers. Measured SC and epidermal thickness compared very well with previous reports from the literature. Over 1,800 readings of the deepest particle edge and size of the particles were made on similar

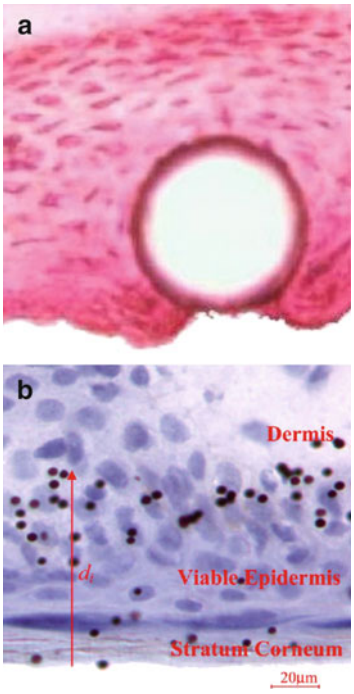

Fig. 7 Photomicrographs of particles delivered to human skin. A 20 μm radius glass sphere delivered at 260 m s^{-1} (**a**) and gold particles (1.0 ± 0.2 μm radius) delivered at 580 ± 50 m s^{-1} (**b**) are shown. From Kendall et al. (2004a)

histological sections with polystyrene, stainless steel and glass particles, selected for different density and size ranges.

In Fig. 7b, a histological section is shown after the impact of gold particles with a measured mean radius of 1 ± 0.2 μm on the skin with a mean calculated impact velocity of 580 ± 50 m s^{-1}. A sample particle depth measurement is labeled as d_i. Over 1,200 readings of the deepest edge and size of the gold particles were made on similar histological sections. All the raw data collected from the histology sections (such as in Fig. 7) are plotted as a function of the particle impact parameter, ρvr, where ρ is the density, v is the velocity and r is the radius, in Fig. 8. The variability of penetration as shown in Fig. 8 is typical of results obtained with other tissues.

Some insights into the sources of scatter in the penetration data of Fig. 8 can be gained when the data are grouped and processed. Consider, for instance, the gold data shown in Fig. 7 grouped by particle radius as shown in Fig. 9. The error bars correspond to one standard deviation in collapsed particle penetration depth and ρvr. Note the trend indicating that for a given value of ρvr, an increase in radius (and hence a decrease in impact velocity) corresponds to a decrease in penetration depth. These data, together with other (unpublished) work show the different particle sizes and the cell matrix results in different penetration depths. For instance, the gold particles are smaller than the average cell size, and during deceleration through the skin tissue, are more likely to penetrate through individual cell membranes. For the larger particles, however, the tissue would primarily fail

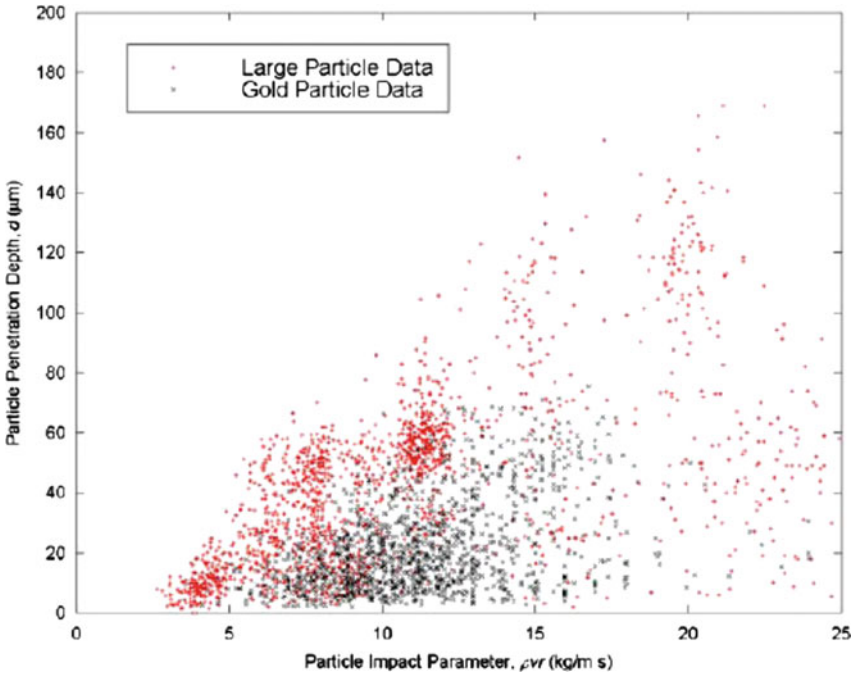

Fig. 8 Raw gold and larger particle penetration into excised human skin as a function of the particle radius, density and impact velocity. From Kendall et al. (2004a)

between the cell boundaries. Indeed, these ballistic penetration data are qualitatively consistent with findings from microprobe indentation studies (Kendall et al. 2007), albeit at considerably higher strain rates.

Corresponding calculated penetration profiles using the theoretical model are also shown in Fig. 9, and illustrate a similar trend with good agreement. Importantly, in this case the yield stress was held constant at 40 MPa, to achieve the closest fit with the data. This is considerably higher than the quasi-static yield stresses reported in the literature (summarized in Table 1 and Fig. 2). This discrepancy is attributed to a huge strain rate effect: the ballistic impact of the microparticle has a peak strain rate of ~10^6 s^{-1}. In a subsequent, more refined study (Kendall et al. 2004b), these strain rate effects are further elucidated.

In addition to the described scale and strain rate effects, another source of variability stems from the high sensitivity in SC mechanical properties to hydration and temperature, deriving from variation in ambient conditions (detailed in Kendall et al. 2004b). Increasing the relative humidity (RH) from 15% to 95% (temperature at 25°C) led to a particle penetration increase by a factor of 1.8. Temperature increases from 20 to 40°C (RH at 15%) enhanced particle penetration two-fold. In both cases, these increases were sufficient to move the target layer from the SC to the VE. In immunotherapeutic applications, this is the difference between the

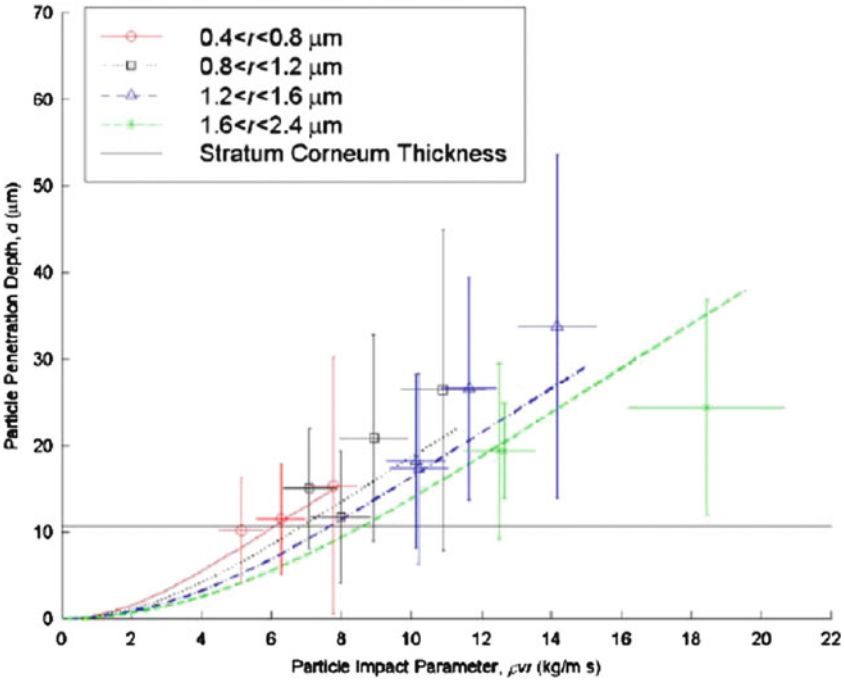

Fig. 9 Impact parameters and penetration depth of gold particles within excised human skin. From Kendall et al. (2004a)

ineffectual delivery of particles to the SC and the targeted delivery of specific cells in the VE.

These collective data show the momentum range obtained from the described biolistic devices primarily translate into delivery within targeted VE and SC. With the precise delivery conditions achieved from these devices, we have obtained new insights into the important biological variability in microparticle impact. This variability, together with more obvious differences in tissue thicknesses (with the tissue site of target, age and gender) must be considered when selecting device conditions for clinical biolistic immunotherapeutic delivery.

4.3.3 Skin Cell Death from Ballistic Impact

The biological responses induced by biolistic impact are of great importance in biolistic applications. When delivered to the tissue surface, the microparticles undergo a tremendous deceleration – peaking at ~10^{10} g – and coming to rest within ~100–200 ns. Such deceleration induces shock and stress waves within the tissue, and it is important to determine under which conditions skin cells are killed. This was investigated in mice, where following the delivery of gold microparticles, the cell death was assayed with mixtures of ethidium bromide and acridine orange

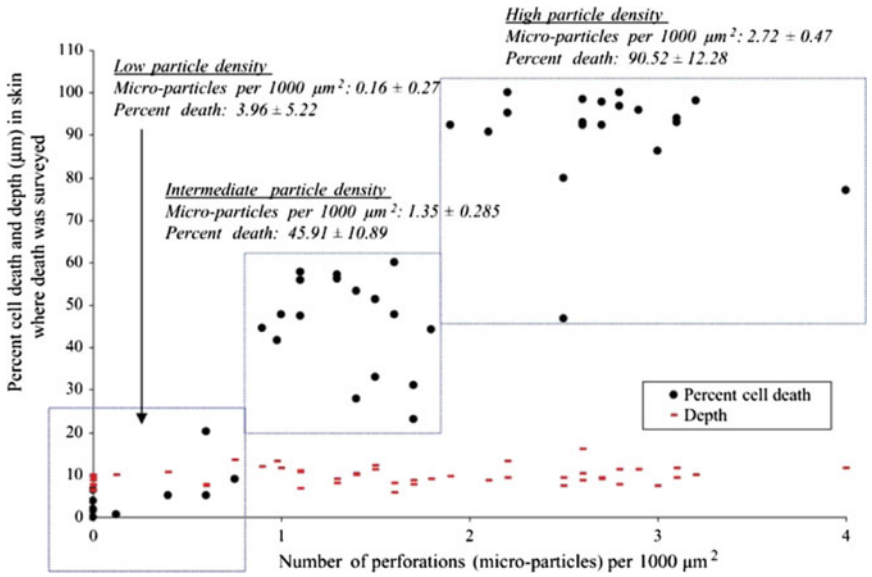

Fig. 10 The viability of epidermal cells targeted by biolistic microparticle delivery (from Raju et al. 2006). Data for this plot was generated by first enumerating the number of perforations per 1,000 μm^2 in the SC caused by microparticle penetration (Fig. 11a). The perforations were equated to microparticles. Second, percent cell death was calculated in the viable epidermis below the stratum corneum using the acridine orange/ethidium bromide assay for discriminating live and dead cells (see Fig. 11b–d)

and imaged non-invasively with Multi-Photon Microscopy (Raju et al. 2006). The data is summarized in Figs. 10 and 11. Each direct impact of a gold microparticle resulted in cell death. Furthermore, even in cases where microparticles passed within ~10 μm of the cell surface – but not touching the cell – cell death resulted. A sufficiently high number density in the tissue can result in complete cell death within the VE. Clearly, this is important when considering the biological responses induced by microparticle impact.

4.4 Clinical Results and Commercial Application

Commercial application. Biolistics is a platform technology for delivering a broad range of drugs and immunotherapeutics. Currently, the technology is progressing commercially in two streams:

- Delivery of lidocaine local anesthetic to the skin (the larger class of particles shown in Fig. 8), approved by the FDA for market application (Zingo™, Anesiva);

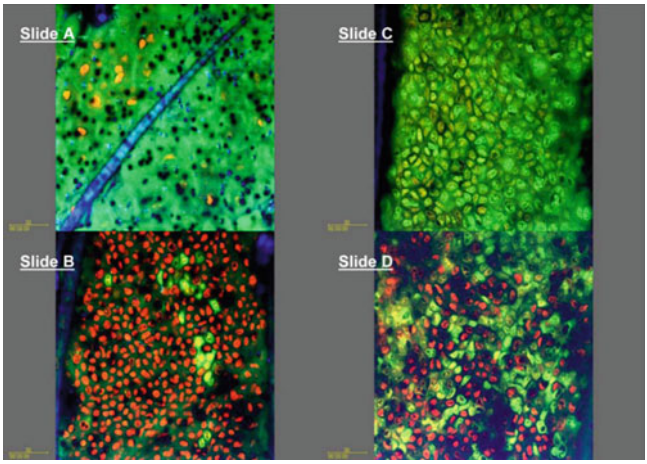

Fig. 11 Murine tissue stained for live–dead cell discrimination with a cocktail of acridine orange/ethidium bromide and imaged with near-infrared two-photon excitation (taken from Raju et al. 2006). Images were collected with LaserSharp software (Carl Zeiss, Hertforshire, UK). Cells emitting red fluorescence are dead whereas cells emitting green fluorescence are alive. (**a**) The dark spots are perforations in the SC caused by microparticle bombardment. (**b**) The corresponding viable epidermis 11.3 μm below the SC. (**a**) and (**b**) represent an image set of "high particle density" shown in Fig. 10. (**c**) The viable epidermis of the control (9.7 μm below the SC) where particle delivery to the tissue was not made. (**d**) Representative of the viable epidermis of tissue with intermediate particle densities (10.5 μm below the SC)

- Delivery of DNA vaccines on gold microparticles (PowderMed^{TM}, Pfizer), undergoing Phase III clinical trials).

Clinical results. Although strong results are achieved in other immunotherapeutics such as allergy immunotherapy of the animal model (Kendall et al. 2006) and lidocaine for anasthesia, the key clinical progress with DNA vaccines is discussed below.

The DNA plasmid that forms the active component of DNA vaccines is precipitated onto microscopic gold particles (typically 2 μg DNA on 1 mg gold). Microscopic elemental gold particles (mean particle diameter ~2 μm) are used as the plasmid DNA carrier, because they are inert and have the appropriate density needed to deliver the vaccine directly into the target epidermal immunologically sensitive cells, including Langerhans cells. Following delivery into the APC, the DNA elutes off the gold particle and is transcribed into RNA. The RNA in turn is translated into the relevant antigen, which is then processed and presented on the cell surface as if it were an intracellular viral protein. An efficient cellular and humoral immune response is thus induced.

A series of clinical trials have been conducted to assess the immunogenicity and safety of a prophylactic hepatitis B virus DNA vaccine (Roy et al. 2000; Rottinghaus et al. 2003; Roberts et al. 2005). These studies have demonstrated that biolistic DNA vaccination can elicit antigen-specific humoral and T cell

responses. In the study by Roy et al. (2000), DNA vaccination with 1–4 μg of hepatitis B surface antigen elicited measurable cytotoxic T cell responses and Th cell responses in 12 healthy adults who had not previously been immunized with a hepatitis B vaccine (Roy et al. 2000). Furthermore, the 12 previously non-vaccinated subjects also seroconverted with levels of hepatitis B-specific antibody ranging from 10 mIU/ml to over 5,000 mIU/ml. This is of particular significance as intramuscular delivery of DNA, using the needle and syringe, with up to 1,000-fold more DNA has generated only low or no antibody responses (MacGregor et al. 1998; MacGregor et al. 2002). The same biolistic hepatitis B DNA vaccine was also shown to increase serum antibody titres in seven of 11 subjects who had previously failed to seroconvert after three or more doses of conventional vaccination with licensed recombinant protein vaccine (Rottinghaus et al. 2003). Finally this plasmid DNA construct has been used to successfully bridge between the earlier bulky experimental device and the simple, hand-held disposable device that will be used for product commercialization (Roberts et al. 2005).

A Phase I study (Drape et al. 2006) has been carried out to investigate the safety and immunogenicity of biolistic administration of an influenza prophylactic plasmid, which encodes a single HA antigen of influenza A/Panama/2007/99 (H3N2). A total of 36 healthy subjects with low pre-existing serological responses to this strain received a vaccination of either 1, 2 or 4 μg DNA at a single administration session. The antibody response was then assessed according to the Committee for Medicinal Products for Human Use (CHMP) criteria for the approval of annual flu vaccines in the European Union. Table 2 summarizes these humoral responses, determined as a haemagglutination inhibition titre elicited on days 0 (predose), 14,

Table 2 Serum antibody responses, seroconversion and seroprotection rate. From Drape et al. (2006)

Group	Day	GMT (range)	Seroconversion[a] (%)	Seroprotection[b] (%)	Mean GMT increase (fold)
1	0	16 (5–40)	–	17 (2/12)	–
	14	23 (5–160)	8 (1/12)	42 (5/12)	1.4
	21	28 (10–240)	17 (2/12)	33 (4/12)	1.7
	56	44 (10–320)	33 (4/12)	58 (7/12)	**2.8**
2	0	17 (5–40)	–	33 (4/12)	–
	14	29 (10–60)	17 (2/12)	50 (6/12)	1.7
	21	36 (20–80)	8 (1/12)	58 (7/12)	2.1
	56	65 (20–320)	**67 (8/12)**	**92 (11/12)**	**3.9**
3	0	12 (5–40)	–	8 (1/12)	–
	14	21 (5–80)	17 (2/12)	25 (3/12)	1.8
	21	40 (10–160)	33 (4/12)	67 (8–12)	3.4
	56	97 (40–640)	**64 (7/11)**	**100 (11/11)**	**8.1**

Values meeting CHMP criteria are bold; geometric mean titer (GMT)

[a]Seroconversion is defined as either a negative pre-vaccination titer ($\leq$10) to a post-vaccination titer $\geq$40, or a significant increase in antibody titer, i.e., at least a four-fold increase between pre- and post-vaccination titers where the pre-vaccination titer is $\geq$10

[b]Seroprotection rate is defined as the proportion of subjects achieving a titer $\geq$40

21 and 56. Time points, where responses met the levels required by the CHMP guidelines for licensing of annual influenza vaccine, are shown in bold.

The 4 μg dose group met the CHMP criteria at day 21, demonstrating the ability of biolistic DNA vaccination to stimulate serological responses equivalent to those seen in protein-based approaches. Furthermore, the responses in all groups continued to increase up to day 56 (the last day monitored) indicating that responses to biolistic vaccination may show a more sustained increase than is typically seen with protein vaccines. By day 56, 100% of those subjects vaccinated with the 4 μg dose were seroprotected.

Overall vaccination was well tolerated and local reactogenicity results were typical of those seen in other biolistic studies.

5 Conclusion

Many vaccines can be radically improved by targeted delivery to particular immunologically-sensitive cells within the outer skin layers. The push is on to develop a range of technologies to meet this need, either using physical or biological targeting approaches. One of these needle-free physical methods, biolistics, delivers biomolecule-coated gold microparticles ballistically to the outer layers of the skin. The method of particle acceleration relies heavily on approaches usually applied to the aerospace industry. Consequently, many unique challenges had to be overcome in engineering biolistic devices for clinical use. Research with the resultant devices has yielded unique insights into the skin at micro-scale dynamic loading – both from mechanical and biological perspectives. Important progress is also being made in clinical trials using biolistic devices to deliver DNA vaccines in the following fields: hepatitis B, influenza, genital herpes, human papilloma virus, HIV/AIDS, Hantaan virus, melanoma and a variety of other cancers.

A newer technology, the Nanopatch (working by a very different principle), is now being developed to address many challenges inherent in the coupling of a ballistic device to skin.

References

Alexander MY, Akhurst RJ (1995) Liposome-medicated gene transfer and expression via the skin. Hum Mol Genet 4:2279–2285

Babiuk S, Baca-Estrada M, Babiuk LA, Ewen C, Foldvari M (2000) Cutaneous vaccination: the skin as an immunologically active tissue and the challenge of antigen delivery. J Control Release 66:199–214

Banchereau J, Steinman RM (1998) Dendritic cells and the control of immunity. Nature 392:245–252

Bauer J, Bahmer FA, Worl J, Neuhuber W, Schuler G, Fartasch M (2001) A strikingly constant ratio exists between Langerhans cells and other epidermal cells in human skin. A stereologic

study using the optical disector method and the confocal laser scanning microscope. J Invest Dermatol 116:313–318
Bellhouse BJ, Sarphie DF, Greenford JC (1994) Needle-less syringe using supersonic gas flow for particle delivery. International patent WO94/24263
Blank IH, Moloney J, 3rd, Emslie AG, Simon I, Apt C (1984) The diffusion of water across the stratum corneum as a function of its water content. J Invest Dermatol 82:188–94
Berman B, Chen VL, France DS, Dotz WI, Petroni G (1983) Anatomical mapping of epidermal Langerhans cell densities in adults. Br J Dermatol 109:553–558
Bremseth DL, Pass F (2001) Delivery of insulin by jet injection: recent observations. Diabetes Technol Ther 3:225–232
Burkoth TL, Bellhouse BJ, Hewson G, Longridge DJ, Muddle AG, Sarphie DF (1999) Transdermal and transmucosal powdered drug delivery. Crit Rev Ther Drug Carrier Syst 16:331–384
Chen D, Endres RL, Erickson CA, Weis KF, McGregor MW, Kawaoka Y, Payne LG (2000) Epidermal immunization by a needle-free powder delivery technology: immunogenicity of influenza vaccine and protection in mice. Nat Med 6:1187–1190
Chen D, Maa YF, Haynes JR (2002) Needle-free epidermal powder immunization. Expert Rev Vaccines 1:265–276
Chen H, Yuan J, Wang Y, Silvers WK (1985) Distribution of ATPase-positive Langerhans cells in normal adult human skin. Br J Dermatol 113:707–711
Chen X, Prow TW, Crichton ML, Jenkins DWK, Roberts MS, Frazer IH, Fernando GJP, Kendall MAF (2009) Dry-coated microprojection array patches for targeted delivery of immunotherapeutics to the skin. J Control Release 3:212–220
Chen XF, Prow TW, Crichton M, Fernando G, Kendall MAF (2008) Novel coating of Micronanoprojections patches for targeted vaccine delivery to skin. In: International Conference on Nanoscience and Nanotechnology, Melbourne Convention Centre, Melbourne, Australia. IEEE Press, pp 105–108
Christensen MS, Hargens CW 3rd, Nacht S, Gans EH (1977) Viscoelastic properties of intact human skin: instrumentation, hydration effects, and the contribution of the stratum corneum. J Invest Dermatol 69:282–286
Cui Z, Mumper RJ (2001) Dendritic cell-targeted genetic vaccines engineered from novel microemulsion precursors. Mol Ther 3:S352
Dehn J (1976) A unified theory of penetration. Int J Impact Eng 5:239–248
Dobrev H (1996) In vivo noninvasive study of the mechanical properties of the human skin after single application of topical corticosteroids. Folia Med (Plovdiv) 38:11–17
Domashenko A, Gupta S, Cotsarelis G (2000) Efficient delivery of transgenes to human hair follicle progenitor cells using topical lipoplex. Nat Biotechnol 18:420–423
Drape RJ, Macklin MD, Barr LJ, Jones S, Haynes JR, Dean HJ (2006) Epidermal DNA vaccine for influenza is immunogenic in humans. Vaccine 24:4475–4481
Duck FA (1990) Physical properties of tissue. Academic Press, London
Fuchs E, Raghavan S (2002) Getting under the skin of epidermal morphogenesis. Nat Rev Genet 3:199–209
Furth PA, Shamay A, Hennighausen L (1995) Gene transfer into mammalian cells by jet injection. Hybridoma 14:149–152
Gill HS, Prausnitz MR (2007) Coating formulations for microneedles. Pharm Res 24:1369–1380
Givens B, Oberle S, Lander J (1993) Taking the jab out of needles. Can Nurse 89:37–40
Glenn GM, Kenney RT, Ellingsworth LR, Frech SA, Hammond SA, Zoeteweij JP (2003) Transcutaneous immunization and immunostimulant strategies: capitalizing on the immunocompetence of the skin. Expert Rev Vaccines 2:253–267
Guerena-Burgueno F, Hall ER, Taylor DN, Cassels FJ, Scott DA, Wolf MK, Roberts ZJ, Nesterova GV, Alving CR, Glenn GM (2002) Safety and immunogenicity of a prototype enterotoxigenic *Escherichia coli* vaccine administered transcutaneously. Infect Immun 70:1874–1880

Hardy MP, Kendall MAF (2005) Mucosal deformation from an impinging transonic gas jet and the ballistic impact of microparticles. Phys Med Biol 50:4567–4580

Hoath SB, Leahy DG (2002) Formation and function of the stratum corneum. In: Marks R, Lévêque J-L, Voegeli R (eds) The essential stratum corneum. Taylor & Francis Group, London, p 31

Hopewell JW (1990) The skin: its structure and response to ionizing radiation. Int J Radiat Biol 57:751–773

Kendall M (2006) Engineering of needle-free physical methods to target epidermal cells for DNA vaccination. Vaccine 24:4651–4656

Kendall M, Mitchell T, Wrighton-Smith P (2004a) Intradermal ballistic delivery of micro-particles into excised human skin for pharmaceutical applications. J Biomech 37: 1733–1741

Kendall M, Mitchell TJ, Costigan G, Armitage M, Lenzo JC, Thomas JA, von Garnier C, Zosky GR, Turner DJ, Stumbles PA, Sly PD, Holt PG, Thomas WR (2006) Downregulation of IgE antibody and allergic responses in the lung by epidermal biolistic microparticle delivery. J Allergy Clin Immunol 117:275–282

Kendall M, Rishworth S, Carter F, Mitchell T (2004b) Effects of relative humidity and ambient temperature on the ballistic delivery of micro-particles to excised porcine skin. J Invest Dermatol 122:739–746

Kendall MA, Chong YF, Cock A (2007) The mechanical properties of the skin epidermis in relation to targeted gene and drug delivery. Biomaterials 28:4968–4977

Kendall MAF (2002) The delivery of particulate vaccines and drugs to human skin with a practical, hand-held shock tube-based system. Shock Waves 12:22–30

Kendall MAF, Quinlan NJ, Thorpe SJ, Ainsworth RW, Bellhouse BJ (2004c) Measurements of the gas and particle flow within a converging–diverging nozzle for high speed powdered vaccine and drug delivery. Exp Fluids 37:128–136

Lesinski GB, Smithson SL, Srivastava N, Chen D, Widera G, Westerink MA (2001) A DNA vaccine encoding a peptide mimic of *Streptococcus pneumoniae* serotype 4 capsular polysaccharide induces specific anti-carbohydrate antibodies in Balb/c mice. Vaccine 19: 1717–1726

Li L, Hoffman RM (1995) The feasibility of targeted selective gene therapy of the hair follicle. Nat Med 1:705–706

Liu LJ, Watabe S, Yang J, Hamajima K, Ishii N, Hagiwara E, Onari K, Xin KQ, Okuda K (2001) Topical application of HIV DNA vaccine with cytokine-expression plasmids induces strong antigen-specific immune responses. Vaccine 20:42–48

Liu Y, Kendall MAF (2004a) Numerical simulation of heat transfer from a transonic jet impinging on skin for needle-free powdered drug and vaccine delivery. Proc Inst Mech Eng – Part C – J Mech Eng Sci 218:1373–1383

Liu Y, Kendall MAF (2004b) Numerical study of a transient gas and particle flow in a high-speed needle-free ballistic particulate vaccine delivery system. J Mech Med Biol 4:559–578

Liu Y, Truong NK, Kendall MA, Bellhouse BJ (2007) Characteristics of a micro-biolistic system for murine immunological studies. Biomed Microdevices 9:465–474

Lu B, Federoff HJ, Wang Y, Goldsmith LA, Scott G (1997) Topical application of viral vectors for epidermal gene transfer. J Invest Dermatol 108:803–808

MacGregor RR, Boyer JD, Ugen KE, Lacy KE, Gluckman SJ, Bagarazzi ML, Chattergoon MA, Baine Y, Higgins TJ, Ciccarelli RB, Coney LR, Ginsberg RS, Weiner DB (1998) First human trial of a DNA-based vaccine for treatment of human immunodeficiency virus type 1 infection: safety and host response. J Infect Dis 178:92–100

MacGregor RR, Ginsberg R, Ugen KE, Baine Y, Kang CU, Tu XM, Higgins T, Weiner DB, Boyer JD (2002) T-cell responses induced in normal volunteers immunized with a DNA-based vaccine containing HIV-1 env and rev. AIDS 16:2137–2143

Marrion M, Kendall MAF, Liu Y (2005) The gas-dynamic effects of a hemisphere-cylinder obstacle in a shock-tube driver. Exp Fluids 38:319–327

Matriano JA, Cormier M, Johnson J, Young WA, Buttery M, Nyam K, Daddona PE (2002) Macroflux microprojection array patch technology: a new and efficient approach for intracutaneous immunization. Pharm Res 19:63–70

McAllister DV, Wang PM, Davis SP, Park JH, Canatella PJ, Allen MG, Prausnitz MR (2003) Microfabricated needles for transdermal delivery of macromolecules and nanoparticles: fabrication methods and transport studies. Proc Natl Acad Sci USA 100:13755–13760

McKinney EC, Streilein JW (1989) On the extraordinary capacity of allogeneic epidermal Langerhans cells to prime cytotoxic T cells in vivo. J Immunol 143:1560–1564

Menton DN, Eisen AZ (1971) Structure and organization of mammalian stratum corneum. J Ultrastruct Res 35:247–264

Mikszta JA, Alarcon JB, Brittingham JM, Sutter DE, Pettis RJ, Harvey NG (2002) Improved genetic immunization via micromechanical disruption of skin-barrier function and targeted epidermal delivery. Nat Med 8:415–419

Mitchell T (2003) The ballistics of micro-particles into the mucosa and skin. DPhill Thesis Engineering science, University of Oxford, Oxford

Mitchell TJ, Kendall MAF, Bellhouse BJ (2003) A ballistic study of micro-particle penetration to the oral mucosa. Int J Impact Eng 28:581–599

Mumper RJ, Ledebur HC Jr (2001) Dendritic cell delivery of plasmid DNA. Applications for controlled genetic immunization. Mol Biotechnol 19:79–95

Nagao K, Ginhoux F, Leitner WW, Motegi S, Bennett CL, Clausen BE, Merad M, Udey MC (2009) Murine epidermal Langerhans cells and langerin-expressing dermal dendritic cells are unrelated and exhibit distinct functions. Proc Natl Acad Sci USA 106:3312–3317

Nemes Z, Steinert PM (1999) Bricks and mortar of the epidermal barrier. Exp Mol Med 31:5–19

Nicolopoulos CS, Giannoudis PV, Glaros KD, Barbenel JC (1998) In vitro study of the failure of skin surface after influence of hydration and preconditioning. Arch Dermatol Res 290:638–640

Numahara T, Tanemura M, Nakagawa T, Takaiwa T (2001) Spatial data analysis by epidermal Langerhans cells reveals an elegant system. J Dermatol Sci 25:219–228

Papir YS, Hsu KH, Wildnauer RH (1975) The mechanical properties of stratum corneum I. The effect of water and ambient temperature on the tensile properties of newborn rat stratum corneum. Biochim Biophys Acta 399:170–180

Poulin LF, Henri S, de Bovis B, Devilard E, Kissenpfennig A, Malissen B (2007) The dermis contains langerin + dendritic cells that develop and function independently of epidermal Langerhans cells. J Exp Med 204:3119–3131

Prow TW, Chen XF, Crichton M, Tiwari Y, Gradissi F, Raphaelli K, Mahony D, Fernando G, Roberts MS, Kendall MAF (2008) Targeted epidermal delivery of vaccines from coated micro-nanoprojection patches. In: International Conference on Nanoscience and Nanotechnology. IEEE, Melbourne Convention Centre, Melbourne, Australia, pp 125–128

Quinlan NJ, Kendall MAF, Bellhouse BJ, Ainsworth RW (2001) Investigations of gas and particle dynamics in first generation needle-free drug delivery devices. Int J Shock Waves 10:395–404

Raju PA, McSloy N, Truong NK, Kendall MA (2006) Assessment of epidermal cell viability by near infrared multi-photon microscopy following ballistic delivery of gold micro-particles. Vaccine 24:4644–4647

Rawlings A, Harding C, Watkinson A, Banks J, Ackerman C, Sabin R (1995) The effect of glycerol and humidity on desmosome degradation in stratum corneum. Arch Dermatol Res 287:457–464

Roberts LK, Barr LJ, Fuller DH, McMahon CW, Leese PT, Jones S (2005) Clinical safety and efficacy of a powdered hepatitis B nucleic acid vaccine delivered to the epidermis by a commercial prototype device. Vaccine 23:4867–4878

Rottinghaus ST, Poland GA, Jacobson RM, Barr LJ, Roy MJ (2003) Hepatitis B DNA vaccine induces protective antibody responses in human non-responders to conventional vaccination. Vaccine 21:4604–4608

Roy MJ, Wu MS, Barr LJ, Fuller JT, Tussey LG, Speller S, Culp J, Burkholder JK, Swain WF, Dixon RM, Widera G, Vessey R, King A, Ogg G, Gallimore A, Haynes JR, Heydenburg Fuller

D (2000) Induction of antigen-specific $CD8^+$ T cells, T helper cells, and protective levels of antibody in humans by particle-mediated administration of a hepatitis B virus DNA vaccine. Vaccine 19:764–778

Sanford JC, Klein MC (1987) Delivery of substances into cells and tissues using a particle bombardment process. Particulate Sci Tech 5:27–37

Shi Z, Curiel DT, Tang DC (1999) DNA-based non-invasive vaccination onto the skin. Vaccine 17:2136–2141

Shi Z, Zeng M, Yang G, Siegel F, Cain LJ, van Kampen KR, Elmets CA, Tang DC (2001) Protection against tetanus by needle-free inoculation of adenovirus-vectored nasal and epicutaneous vaccines. J Virol 75:11474–11482

Sintov AC, Krymberk I, Daniel D, Hannan T, Sohn Z, Levin G (2003) Radiofrequency-driven skin microchanneling as a new way for electrically assisted transdermal delivery of hydrophilic drugs. J Control Release 89:311–320

Stenn KS, Goldenhersh MA, Trepeta RW (1992) Structure and functions of the skin. In: Symmers WSC (ed) The skin, Vol 9. New York, Churchill Livingstone, pp 1–14

Tang DC, Shi Z, Curiel DT (1997) Vaccination onto bare skin. Nature 388:729–730

Timares L, Takashima A, Johnston SA (1998) Quantitative analysis of the immunopotency of genetically transfected dendritic cells. Proc Natl Acad Sci USA 95:13147–13152

Truong NK, Liu Y, Kendall MAF (2006) Gas-particle dynamics characterisation of a preclinical contoured shock tube for vaccine and drug delivery. Shock Waves 15:149–164

Watabe S, Xin KQ, Ihata A, Liu LJ, Honsho A, Aoki I, Hamajima K, Wahren B, Okuda K (2001) Protection against influenza virus challenge by topical application of influenza DNA vaccine. Vaccine 19:4434–4444

WHO (1999) Safety of injections: facts and figures. http://www.who.int/inf-fs/en/fact232.html World Health Organization. Office of Press and Public Relations

Widera G, Austin M, Rabussay D, Goldbeck C, Barnett SW, Chen M, Leung L, Otten GR, Thudium K, Selby MJ, Ulmer JB (2000) Increased DNA vaccine delivery and immunogenicity by electroporation in vivo. J Immunol 164:4635–4640

Wildnauer RH, Bothwell JW, Douglass AB (1971) Stratum corneum biomechanical properties I. Influence of relative humidity on normal and extracted human stratum corneum. J Invest Dermatol 56:72–78

Zucchelli S, Capone S, Fattori E, Folgori A, Di Marco A, Casimiro D, Simon AJ, Laufer R, La Monica N, Cortese R, Nicosia A (2000) Enhancing B- and T-cell immune response to a hepatitis C virus E2 DNA vaccine by intramuscular electrical gene transfer. J Virol 74:11598–11607